

# SUOD: A Scalable Unsupervised Outlier Detection Framework

Yue Zhao  
zhaoy@cmu.edu  
Carnegie Mellon University

Xiyang Hu  
xiyanghu@cmu.edu  
Carnegie Mellon University

Cheng Cheng  
ccheng2@andrew.cmu.edu  
Carnegie Mellon University

Cong Wang  
wangcong@cmu.edu  
Carnegie Mellon University

Cao Xiao  
cao.xiao@iqvia.com  
Analytics Center of  
Excellence, IQVIA

Yunlong Wang  
yunlong.wang@iqvia.com  
Department of Advanced  
Analytic, IQVIA

Jimeng Sun  
jimeng@illinois.edu  
University of Illinois at  
Urbana-Champaign

Leman Akoglu  
lakoglu@andrew.cmu.edu  
Carnegie Mellon University

## ABSTRACT

Outlier detection is a key data mining task for identifying abnormal objects from massive data. Due to the high expense of acquiring ground truth, practitioners lean towards building a large number of unsupervised models for further combination and analysis, rather than relying on a single model out of reliability consideration. However, this poses scalability challenge to high-dimensional, large datasets. In this study, we propose a three-module framework called SUOD (Scalable Unsupervised Outlier Detection) to address the challenge. It can accelerate outlier model building and scoring when a large number of base models are used. It focuses on three complementary levels to speed up the process while controlling prediction performance degradation at the same time. At the **data level**, its Random Projection module projects high-dimensional data onto diversified low-dimensional subspaces while preserving the pairwise distance relationship. At the **model level**, SUOD's Pseudo-supervised Approximation module can approximate and replace fitted unsupervised models by low-cost supervised regressors, leading to fast offline scoring on new-coming samples with better interpretability. At the **system level**, Balanced Parallel Scheduling module mitigates the workload imbalance within distributed systems, which is helpful for heterogeneous outlier ensembles.

As the three modules are independent with different focuses (data dimensionality, inference efficiency, and task load balance), they have great flexibility to “mix and match”. The framework is also designed with customizability and extensibility in mind. One may customize each module based on specific use cases, and the framework may be generalized to other learning tasks as well, e.g., streaming-based outlier detection and clustering. Extensive experiments on more than 20 benchmark datasets demonstrate SUOD's effectiveness. In addition, a real-world deployment system on fraudulent claim analysis by IQVIA is also discussed. The full framework, documentation, and examples are openly shared and can be accessed at <https://github.com/yzhao062/SUOD>.

## KEYWORDS

Outlier Detection, Scalability, Machine Learning Systems

### ACM Reference Format:

Yue Zhao, Xiyang Hu, Cheng Cheng, Cong Wang, Cao Xiao, Yunlong Wang, Jimeng Sun, and Leman Akoglu. 2020. SUOD: A Scalable Unsupervised Outlier Detection Framework. In *Proceedings of the 26th ACM SIGKDD*

*International Conference on Knowledge Discovery and Data Mining (KDD'20)*. ACM, New York, NY, USA, Article 4, 10 pages. [https://doi.org/10.475/123\\_4](https://doi.org/10.475/123_4)

## 1 INTRODUCTION

Outlier detection aims at identifying the samples that are deviant from the general data distribution [36], which has been used in various applications [10]. Notably, most of the existing outlier detection algorithms are unsupervised due to the high cost of acquiring ground truth [35]. However, using a single unsupervised model is risky by nature, and using a large group of unsupervised models with variations are therefore recommended, e.g., different algorithms, varying parameters, distinct views of the datasets, etc [4]. Outlier ensemble methods that select and combine diversified base detectors can be useful in this content [2, 4, 37], and more reliable results may be achieved. For industry applications, a single model solution will not go through due to (i) the limited knowledge of the underlying data and (ii) operational (even “political”) considerations—multiple models must be explored before the final decision can be made. The simplest combination is to take the average or maximum across all the base detectors as the final result [4], along with more complex combination approaches in both unsupervised [35] and semi-supervised manners [34].

However, training and scoring new samples with a large number of base models can be computationally expensive on high-dimensional, large datasets. For instance, proximity-based algorithms, assuming outliers behave differently in specific regions [3], can be prohibitively slow or even completely fail to work under this setting. For instance, representative methods including  $k$  nearest neighbors ( $k$ NN) [27], local outlier factor (LOF) [9], and local outlier probabilities (LoOP) [16], operate in Euclidean space for distance/density calculation, suffering from the curse of dimensionality [29]. Numerous works have attempted to tackle this scalability challenge from various angles, e.g., projection [15], subspace [20], and distributed learning [22, 25]. **However, none of them provides a comprehensive solution by considering multiple aspects, leading to limited generalization ability and efficacy.**

To tap the gap, we propose an end-to-end acceleration framework called SUOD (Scalable Unsupervised Outlier Detection), which has gained recognition from both academia [33] and industry<sup>1</sup> since its inception. As shown in Fig. 1, SUOD has three modules focusing on complementary levels: random projection (**data level**), pseudo-supervised approximation (**model level**), and balanced parallel

<sup>1</sup>By the submission time, it has been downloaded by more than 120,000 times on PyPI.

scheduling (**system level**). For high-dimensional data, SUOD generates a random low-dimensional subspace for each base model by Johnson-Lindenstrauss projection [14], in which the corresponding base model is trained. If scoring new-coming samples by anomalousness is needed, more efficient supervised regressors are employed to approximate complex unsupervised outlier detectors. The supervised models are trained with “pseudo ground truth”, i.e., the predicted outlier scores generated by the unsupervised models on the train set. The rationale behind is that supervised models are faster for prediction and more interpretable; it may be viewed as distilling knowledge from unsupervised models [11]. The attention is also given to the acceleration in distributed systems, as most industry applications take this route. Specifically, we design a balanced parallel scheduling mechanism to address scheduling inefficiency in distributed systems, which happens to heterogeneous base models with drastic time-complexity difference (e.g.,  $k$ NN can take much longer time to run than isolation based techniques). We propose to forecast the running time of each base model before scheduling so that the task load could be evenly distributed among workers. Notably, all three acceleration modules are designed to be fully independent but complementary. They can be either used alone or combined as a framework. It is noted that SUOD is designed for offline learning with a stationary assumption, and may be extended to online settings for streaming data.

Our contributions could be summarized as follows:

- (1) Examine the impact of various projection methods in outlier detection and identify the method(s) for simultaneous dimensionality reduction and diversity induction.
- (2) Analyze pseudo-supervised regression models’ performance in approximating unsupervised outlier detectors. To our best knowledge, this is the first research effort toward leveraging distillation for unsupervised outlier detection.
- (3) Fix an imbalance scheduling issue in distributed systems for heterogeneous detectors, with time reduction up to 61%.
- (4) Conduct extensive experiments to show the effectiveness of the three acceleration experiments independently, and of the entire framework as a whole, along with a real-world deployment case on claim fraud detection by IQVIA.

In summary, SUOD has the following properties: (i) effective dimensionality reduction and diversity induction by Johnson-Lindenstrauss projection; (ii) faster and more interpretable new-coming point scoring via model approximation and (iii) efficient parallel training and scoring by load-balanced task scheduling. With all these instruments, the proposed SUOD framework can facilitate large-scale applications in security, healthcare, finance, etc.

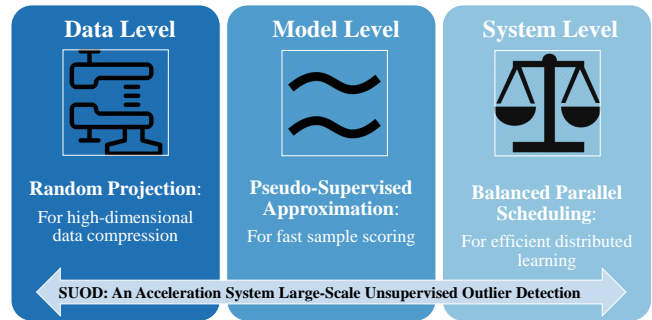
## 2 RELATED WORKS

### 2.1 Outlier Detection and Ensemble Learning

Outlier detection has numerous important applications in various fields, such as rare disease detection [19], healthcare utilization analysis [12], video surveillance [23], fraudulent online review analysis [5], and network intrusion detection [17]. Yet, detecting outliers is a challenging task due to various reasons [2, 35, 36].

Most of the existing detection algorithms are unsupervised as ground truth is often absent in practice, and acquiring labels can be prohibitively expensive. Consequently, practitioners tend to rely on

Figure 1: SUOD’s three-level design chart



established unsupervised outlier detection algorithms like Isolation Forest [20], Local Outlier Factor (LOF) [9], and Angle-based Outlier Detection (ABOD) [16]. Regarding unsupervised neural models like autoencoders and generative adversarial networks [21], the limited amount of data curbs the effectiveness of representation learning. Hence, no single outlier detection model could always outperform, and it is hard to assess the performance without ground truth.

Therefore, relying on a single unsupervised model has inherently high risk, and outlier ensembles that leverage a group of detectors have become increasingly popular [2, 4, 37]. There are a group of unsupervised outlier ensemble frameworks proposed in the last several years from simple average, maximization, weighted average, second-phase combination methods [4] to more complex selective models like SELECT [28] and LSCP [35]. Although unsupervised outlier ensemble methods can be effective in certain cases, they could not incorporate the existing ground truth information regardless of its richness. As a result, a few semi-supervised detection frameworks that combine existing labels with unsupervised data representation are proposed recently [24, 34]. For both unsupervised and semi-supervised outlier ensemble methods, a large group of diversified unsupervised base detectors should be trained as the first step—SUOD is hereby proposed to accommodate this need.

### 2.2 Scalability Challenges in Outlier Detection

Efforts have been made through various channels to accelerate large-scale outlier detection. On the **data level**, researchers try to project high-dimensional data onto lower-dimensional subspaces [1], including simple Principal Component Analysis (PCA) [30] and more complex subspace method HiCS [15]. However, deterministic projection methods, e.g., PCA, are fast but not ideal for building diversified base detectors for outlier ensembles—it leads to the same or similar subspaces with limited diversity by nature, which results in the loss of outliers [3]. Complex projection and subspace methods may bring performance improvement for outlier mining, but the generalization capacity is limited. Hence, projection methods preserving pairwise distance relationships for downstream operations should be considered. Beyond preserving pairwise relationship, SUOD’s also considers diversity induction for downstream tasks, leading to both meaningful but diversified feature spaces (see 3.1).

On the **model level**, knowledge distillation emerges as a good way of compressing large neural networks recently [11], while its

usage in outlier detection is still underexplored. Knowledge distillation refers to the notion of compressing an ensemble of large, often cumbersome model(s) into a small and more interpretable one(s). A similar idea may be adapted to outlier mining by coupling supervised and unsupervised models. Specifically, proximity-based models, such as LOF, can be slow (high time complexity) to score on new-coming data samples. Meanwhile, unsupervised non-parametric models lack interpretability, which severely restricts their usability in practice. It is noted that SUOD shares a similar concept as knowledge distillation for computational cost optimization but comes with a few fundamental differences (see §3.2).

Software engineering cures have been explored as well on the **system level**—model training and prediction can be expedited through parallelization with multiple workers (e.g., CPU cores) [22, 25]. However, existing distributed frameworks can be inefficient if training and prediction task assignments are not balanced among workers. That is, a group of heterogeneous detection models can have significantly different computational cost. As a simple example, let us split 100 heterogeneous models into 4 groups for parallel training. If group #2 takes significantly longer time than the others to finish, it will behave like the bottleneck of the system. More formally, the imbalanced task scheduling amplifies the impact of slower worker(s); the system efficiency is curbed by the slowest group. As shown in §3.3, the general parallel task scheduling algorithms in popular machine learning frameworks like scikit-learn [26] is inefficient under this setting, which can be improved.

### 3 FRAMEWORK DESIGN

The proposed SUOD framework contains three independent modules. As shown in Fig. 1 and Algorithm 1, each module is enabled only if the corresponding conditions are met. For high-dimensional data, SUOD randomly projects the original feature onto low-dimensional spaces (§3.1). Pairwise distance relationships are expected to be maintained, and the diversity should be induced for further combination. If scoring on new samples is needed, an efficient supervised regressor may be initialized to approximate the output of each costly unsupervised detector, and the original detectors are no longer needed (§3.2). To expedite the training and offline scoring with a large number of heterogeneous models, we propose a balanced scheduling mechanism (§3.3) to utilize the resource efficiently.

SUOD's API design is inspired by scikit-learn and PyOD; it follows an initialization, fit, and prediction schema, as shown in Code Snippet 1.

#### 3.1 Data Level: Random Projection (RP)

A widely used projection algorithm for high-dimensional data is the Johnson-Lindenstrauss (JL) projection [14], which has been applied to outlier detection recently because of its great scalability [29]. Unlike PCA discussed in §2.2, JL projection could compress the data without heavy distortion on the Euclidean space—outlyingness information is therefore preserved in the compression. Moreover, its built-in randomness can be extremely useful for diversity induction.

This linear transformation is defined as: given a set of data  $X = \{x_1, x_2, \dots, x_n\}$ , each  $x_i \in \mathbb{R}^d$ , let  $W$  be a  $d \times k$  matrix with each entry drawing independently from a predefined distribution like  $\mathcal{N}(0, 1)$ . Then the JL projection is a function  $f : \mathbb{R}^d \rightarrow \mathbb{R}^k$  such that

---

#### Algorithm 1 Scalable Unsupervised Outlier Detection

---

**Inputs:** a group of  $m$  unsupervised outlier detectors  $\mathcal{D}$ ;  $d$  dimension training data  $X_{train}$  and test data  $X_{test}$  (optional); projection threshold  $\theta$ ; target dimension  $k$ ; pre-trained cost predictor  $C_{cost}$ ; # of workers  $t$

**Outputs:** fitted unsupervised models  $\mathcal{D}$ ; fitted pseudo-supervised regressors  $\mathcal{R}$  (optional); test prediction results  $\hat{y}_{test}$  (optional)

- 1: **for** Each detector  $\mathcal{D}_i$  in  $\mathcal{D}$  **do**
- 2:     **if**  $d > \theta$  **then**                             // enable random projection
- 3:         Generate random subspace  $\psi_i$  with dimension of  $k$  by JL projection on  $X_{train}$  (§3.1)
- 4:     **else**  $d < \theta$                                  // disable random projection
- 5:         Use the original feature space  $\psi_i := X_{train}$
- 6:     **end if**
- 7: **end for**
- 8: **if** # of workers  $t \geq 2$  **then**             // parallel learning activated
- 9:     Train each  $\mathcal{D}_i$  on the corresponding  $\psi_i$  by Balanced Parallel Scheduling (§3.3) on  $t$  workers (Eq. (2) and Fig. 2)
- 10: **end if**
- 11: **Return**  $\mathcal{D}$
- 12: **if**  $X_{test} \neq \text{None}$  **then**             // model approximation activated
- 13:     Acquire the pseudo ground truth  $target^{\psi_i}$  as the output of  $\mathcal{D}_i$  on  $\psi_i$ :  $target^{\psi_i} := \mathcal{D}_i(\psi_i)$
- 14:     **for** Each detector  $\mathcal{D}_i$  in  $\mathcal{D}$  **and** approx. flag == True **do**
- 15:         // Expedite loop by Balanced Parallel Scheduling (§3.3)
- 16:         Initialize a supervised regressor  $\mathcal{R}_i$
- 17:         Fit  $\mathcal{R}_i$  by  $\{\psi_i, target^{\psi_i}\}$  by PSA (§3.2)
- 18:          $\hat{y}_{test}^i = \mathcal{R}_i.predict(X_{test})$  // scoring by approximators
- 19:     **end for**
- 20:     **Return**  $\hat{y}_{test}$  and fitted regressors  $\mathcal{R}$
- 21: **end if**

---

$f(x_i) = \frac{1}{\sqrt{k}} W x_i$ . JL projection randomly projects high-dimensional data to lower-dimensional subspaces, but preserves the distance relationship between points. In fact, if we fix some  $v \in \mathbb{R}^d$ , and let  $W$  be the  $k \times d$  matrix such that each entry is from  $\mathcal{N}(0, 1)$ . For every  $\epsilon \in (0, 3)$ , we have [29]:

$$P \left[ (1 - \epsilon) \|v\|^2 \leq \left\| \frac{1}{\sqrt{k}} W v \right\|^2 \leq (1 + \epsilon) \|v\|^2 \right] \leq 2e^{-\epsilon^2 \frac{k}{6}} \quad (1)$$

Fix  $v$  to be the differences between vectors. Then, the above bound shows that for a finite set of  $N$  vectors  $X = \{x_1, x_2, \dots, x_n\} \subseteq \mathbb{R}^d$ , the pairwise Euclidean distance is preserved within a factor of  $(1 \pm \epsilon)$ , given reducing the vectors to  $k = O(\frac{\log(N)}{\epsilon^2})$  dimensions.

Four JL projection variants are considered in this study: (i) *basic*: the transformation matrix is generated by standard Gaussian; (ii) *discrete*: the transformation matrix is picked randomly from Rademacher distribution (uniform in  $\{-1, 1\}$ ); (iii) *circulant*: the transformation matrix is obtained by rotating the subsequent rows from the first row which is generated from standard Gaussian and (iv) *toeplitz*: the first row and column of the transformation matrix are generated from standard Gaussian, and each diagonal uses a constant value from the first row and column. A more thorough empirical study on JL methods can be found in [32].

**Code Snippet 1: Demo of SUOD API**

```

>>> from suod.models.base import SUOD
      # initialize a group of base detectors
>>> base_estimators = [
      LOF(n_neighbors=40), ABOD(n_neighbors=50),
      LOF(n_neighbors=60), IForest(n_estimators=100)]
>>> # initialize SUOD model with module flags
>>> clf = SUOD(base_estimators=base_estimators,
      rp_flag_global=True, approx_clf=approx_clf,
      bps_flag=True, approx_flag_global=True)
>>> # fit and make prediction
>>> clf.fit(X_train)
>>> y_test_labels = clf.predict(X_test)
>>> y_test_scores = clf.decision_function(X_test)

```

Let  $X \in \mathcal{R}^{n \times d}$  denote a dataset with  $n$  points and  $d$  features. The projection module is only invoked if the data dimension exceeds dimension threshold  $\theta$ , and then reduces the original dimension to the target dimension  $k$ . That is, SUOD checks whether  $d$  is higher than the projection threshold  $\theta$ . If so, a JL transformation matrix  $W \in \mathcal{R}^{d \times k}$  is initialized by one of the JL projection methods, and  $X$  is projected onto the  $k$  dimension subspace by  $W$ . Nonetheless, RP module should be used with caution. First, projection may be less useful or even detrimental for subspace methods like Isolation Forest and HBOS. Second, if the number of samples  $n$  is too small, the above JL bound does not hold—the result may be less stable.

### 3.2 Model Level: Pseudo-Supervised Approximation (PSA)

Once the unsupervised models are fitted on the reduced feature space (see §3.1) or the original space (if no random projection is performed), SUOD can approximate and replace each **costly unsupervised model** by a **faster supervised regressor for scoring on new-coming samples in an offline fashion**. It is worth mentioning that not all unsupervised models need replacing but only the costly ones. For instance, fast algorithms like Isolation Forest and HBOS should not be approximated. It is mainly designed for methods with high time complexity, e.g.,  $k$ NN and LOF. They are slow in scoring new-coming samples (upper bounded by  $\Theta(nd)$ ), and can be effectively replaced by fast supervised models like random forest (upper bounded by  $\Theta(ph)$  where  $p$  denotes the number of base trees and  $h$  denotes the max depth of a tree). This “pseudo-supervised” model uses the output of unsupervised models (outlyingness score) as “the pseudo ground truth”—the goal is to approximate the decision boundaries of the underlying unsupervised model. Ensemble-based tree models are recommended to be used to approximate for their outstanding scalability, robustness to overfitting, and interpretability (e.g., feature importance) [13]. The bottom line is the chosen approximator’s inference cost should be less than the underlying unsupervised model, while maintaining a comparable level of scoring accuracy on new-coming samples.

Notably, this process can also be viewed as using supervised regressors to distill knowledge from unsupervised models. However, our approximation is different from the established knowledge distillation in three aspects. First, our approximation works in a

fully unsupervised manner, unlike the classic distillation under supervised settings. Second, our “teacher” and “student” models have totally different architectures with little to no similarity. Specifically, we recommend using random forest [8] to approximate LOF (a proximity-based density estimation model). Third, our approximation clearly improves interpretability, whereas the student models in neural networks may not.

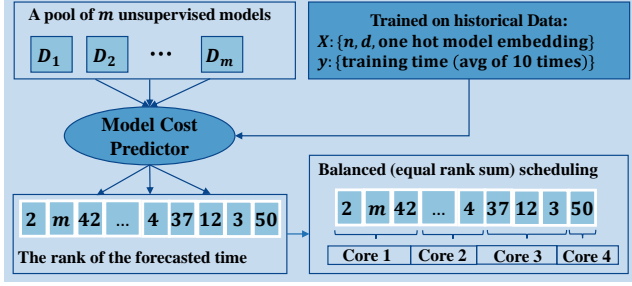
As shown in Algorithm 1, for each trained unsupervised model  $\mathcal{D}_i$ , a supervised regressor  $\mathcal{R}_i$  might be built by using the pseudo ground truth (the output of  $\mathcal{D}_i$ ) as  $y$ .  $\mathcal{D}_i$  is replaced, and the scoring on unseen data will then be made by  $\mathcal{R}_i$  instead. In addition to the execution time reduction, supervised models generally show better interpretability compared with unsupervised counterparts. For instance, random forest used in the experiments can yield feature importance automatically to facilitate understanding. It is noted that although PSA is designed for offline setting, it could be modified for streaming prediction by building a one-class classifier, which is planned to be extended in the next step.

### 3.3 System Level: Balanced Parallel Scheduling (BPS)

BPS aims for assigning model training and scoring (prediction) more evenly across all available workers by model cost. For instance, one may train 25 detectors with varying parameters from each of the four algorithm groups { $k$ NN, Isolation Forest, HBOS, OCSVM}, resulting in 100 models in total. The existing parallel frameworks, e.g., the voting machine in scikit-learn [26], will simply split the models into 4 subgroups by order and schedule the first 25 models (all  $k$ NNs) on Core 1 (worker 1), the next 25 models on Core 2, etc. This does not account for the fact that within a group of heterogeneous detectors, the computational cost varies. Scheduling the task with the equal number of models can result in highly imbalanced tasks. In the worst-case scenario, one worker may be significantly slower than the rest, resulting in halt to the entire process. In this example, the  $k$ NN subgroup will be the system curb. Obviously, this problem applies to both training and scoring stage. One fix is to shuffle the base models randomly. However, there is no guarantee this heuristic could work, and it may be practically infeasible.

The proposed BPS heuristic focuses on designing a more balanced schedule among workers. Ideally, all workers can finish the scheduled tasks within a similar duration and return the results. As shown in Fig. 2, a *model cost predictor*  $C_{cost}$  is built to forecast the model running time (sum of 10 trials) given the input data size, input data dimension, and the algorithm embedding (one-hot). Given the time and resource limitation, a training set with 11 algorithms on 47 benchmark datasets is built, and a random forest regressor [8] is trained on the dataset with 10-fold cross-validation. Although the fitted regressor does not have a high  $R^2$  score, the Spearman’s Rank correlation [31] consistently shows high value ( $r_s > 0.9$ ) with low p-value ( $p < 0.0001$ ). This implies that even if the cost predictor  $C_{cost}$  could not predict the running time precisely, it can predict the rank of the running time with high accuracy. As a result, a scheduling heuristic is proposed by enforcing a nearly equal sum of the rank on running time. Given  $m$  models to be trained, cost predictor  $C_{cost}$  is first invoked to forecast the time cost for a given model  $\mathcal{D}_i$  in  $\mathcal{D}$  as  $C_{cost}(\mathcal{D}_i)$ . After the prediction is done, the predicted

Figure 2: Flowchart of Balanced Parallel Scheduling



time is converted to the rank in  $[1, m]$ . If there are  $t$  cores (workers), each worker will be assigned a group of models to achieve the objective of minimizing the workload imbalance among workers (Eq. 2). So each group has a rank sum at around  $\frac{m^2+m}{2t}$ . Indeed, the accurate running time prediction is less relevant as it depends on the hardware—the rank is more useful as a relevance measure with the transferability to other hardware. That is, the running time will vary on different machines, but the relative rank should preserve. One issue around the sum of ranks is the overestimation of high-rank models. For instance, rank  $f$  model will be counted  $f$  times more heavily than rank 1 model for the sum calculation, even their actual running time difference will not be as big as  $f$  times. To fix this, we introduce a discounted rank by rescaling model rank  $f$  to  $1 + \frac{\alpha f}{m}$ , where  $\alpha$  denotes the scaling strength (default to 1).

$$\min_{\mathcal{W}} \sum_{i=1}^t \left| \sum_{D_j \in \mathcal{W}_i} C_{cost}(D_j) - \sum_{l=1}^m C_{cost}(D_l) \right| \quad (2)$$

It is noted that building multiple large neural networks is rare in outlier detection due to computational consideration. Therefore, the model cost predictor only covers the major methods in Python Outlier Detection Toolbox (PyOD) [36]. For unseen models, they are classified as “unknown” to be assigned with the max cost.

## 4 NUMERICAL EXPERIMENTS & DISCUSSION

First, three experiments are conducted to understand the effect of individual modules independently: (i) **Q1**: how will different RP methods affect the performance of downstream outlier detection (§4.1); (ii) **Q2**: under which conditions (# of models, # of workers etc.), the proposed BPS outperforms the baseline (§4.2) and (iii) **Q3**: will PSA lead to degraded prediction performance compared to the unsupervised detectors (§4.3). Then, the full framework with all three modules enabled is compared with the baseline regarding time cost and scoring accuracy on new samples (§4.4). Finally, a real-world deployment case on fraudulent claim analysis by IQVIA, one of the world largest healthcare research organizations, is described (§4.5). The details of experiment setting, datasets, and evaluation metrics can be found in Appendix A.

### 4.1 Q1: The Comparison among RP Methods

To evaluate the effect of projection, we choose three costly outlier detection algorithms (ABOD, LOF, and  $k$ NN) to measure their execution time, ROC, and P@N, before and after projection. All three detection methods directly or indirectly measure sample similarity in Euclidean space, e.g., pairwise distance, which is prone to the curse of dimensionality and projection may be particularly helpful.

Table 1 shows the comparison among four JL projection variations (see §3.1 for details of *basic*, *discrete*, *circulant*, and *toeplitz*) with **original** (no projection), **PCA**, and **RS** (randomly select  $k$  features from the original  $d$  features, used in Feature Bagging [18] and LSCP [35]). First, all projection methods show superiority regarding time cost. Second, using RS method comes with high instability—it rarely performs the best, which agrees with the findings by Zhao et al. [35]. Third, PCA is always slightly faster than JL projection methods, although the detector performance is inferior to **original** when PCA projection is used along with LOF (Table 1e, 1f, and 1g). The observation supports our claim that PCA is not suited in this scenario (see §2.2). Fourth, JL methods generally lead to equivalent or better prediction performance regarding both ROC and P@N. Lastly, among all four JL methods, *circulant* and *toeplitz* outperform in most cases, and are recommended as default RP methods.

### 4.2 Q2: The Time Reduction Effect of BPS

To evaluate the effectiveness of the proposed BPS algorithm, we run the following experiments by varying: (i) the size ( $n$ ) and the dimension ( $d$ ) of the datasets, (ii) the number of estimators ( $m$ ) and (iii) the number of CPU cores ( $t$ ). The time elapsed is measured in seconds. Due to the space limit, we only show the comparison between the simple scheduling and BPS on **Cardio**, **Letter**, **PageBlock**, and **Pendigits**, by setting  $m \in \{100, 500\}$  and  $t \in \{2, 4, 8\}$ .

Table 2 shows that the proposed BPS has a clear edge over the simple scheduling mechanism (denoted as **Simple** in the tables) that equally splits the tasks by order. It yields a significant time reduction (denoted as % **Redu** in the table), and gets more remarkable if more cores are used along with large datasets. For instance, the time reduction is more than 40% on **PageBlock** and **Pendigits** when 8 cores are used. This agrees with our assumption as model cost should vary more drastically on large datasets if the time complexity is not linear—the proposed BPS method is particularly helpful in this scenario.

### 4.3 Q3: The Visual and Quantitative Analysis of PSA

To better understand the effect of PSA, we first generate 200 synthetic points with Normal distribution for outliers (40 points) and Uniform distribution for normal samples (160 points). In Fig. 3, we plot the decision surfaces of unsupervised models and their corresponding supervised approximators (random forest regressor). It is clear that the decision surfaces change and some regularization effect appears (lower errors on Feature Bagging and  $k$ NN). One assumption is that the approximation process improves the generalization ability of the model by “ignoring” the overfitted points. This fails to work with ABOD because it has an extremely coarse decision surface to approximate (Fig. 3, subfigure 1).

**Table 1: Comparison of various projection methods on different outlier detectors and datasets. Each column corresponds to an evaluation metric; the best performing method is indicated in bold.**

(a) ABOD on MNIST				(b) ABOD on Satellite				(c) ABOD on Satimage-2				(d) ABOD on Cardio			
Method	Time	ROC	P@N	Method	Time	ROC	P@N	Method	Time	ROC	P@N	Method	Time	ROC	P@N
original	12.89	0.80	<b>0.39</b>	original	4.03	0.59	0.41	original	3.68	0.85	0.28	original	0.98	0.59	0.25
PCA	8.93	<b>0.81</b>	0.37	PCA	<b>3.01</b>	0.62	0.44	PCA	<b>2.70</b>	0.88	0.30	PCA	<b>0.82</b>	0.59	0.26
RS	<b>8.27</b>	0.74	0.32	RS	3.53	0.63	0.44	RS	3.20	0.89	0.28	RS	0.92	<b>0.63</b>	<b>0.29</b>
<i>basic</i>	8.94	0.80	0.38	<i>basic</i>	3.10	0.64	0.45	<i>basic</i>	2.78	0.91	0.29	<i>basic</i>	0.83	0.62	0.28
<i>discrete</i>	8.86	0.80	<b>0.39</b>	<i>discrete</i>	3.12	0.65	0.46	<i>discrete</i>	2.79	0.91	<b>0.31</b>	<i>discrete</i>	<b>0.82</b>	0.62	0.28
<i>circulant</i>	9.33	0.80	0.38	<i>circulant</i>	3.14	<b>0.66</b>	<b>0.48</b>	<i>circulant</i>	2.85	0.91	0.29	<i>circulant</i>	0.83	0.62	0.27
<i>toeplitz</i>	8.96	0.80	0.38	<i>toeplitz</i>	3.14	<b>0.66</b>	0.47	<i>toeplitz</i>	2.83	<b>0.92</b>	0.30	<i>toeplitz</i>	0.83	0.62	0.28

(e) LOF on MNIST				(f) LOF on Satellite				(g) LOF on Satimage-2				(h) LOF on Cardio			
Method	Time	ROC	P@N	Method	Time	ROC	P@N	Method	Time	ROC	P@N	Method	Time	ROC	P@N
original	7.64	0.68	0.29	original	0.82	<b>0.55</b>	0.37	original	0.79	0.54	0.07	original	0.08	0.55	0.17
PCA	4.92	0.67	0.27	PCA	<b>0.23</b>	0.54	0.36	PCA	<b>0.20</b>	0.52	0.04	PCA	<b>0.04</b>	0.56	0.19
RS	<b>3.65</b>	0.63	0.23	RS	0.39	0.54	0.37	RS	0.37	0.53	0.08	RS	<b>0.04</b>	0.57	0.15
<i>basic</i>	4.87	0.70	0.31	<i>basic</i>	0.31	0.54	0.37	<i>basic</i>	0.29	0.52	0.08	<i>basic</i>	<b>0.04</b>	<b>0.60</b>	0.20
<i>discrete</i>	5.21	0.70	<b>0.32</b>	<i>discrete</i>	0.32	0.54	0.37	<i>discrete</i>	0.30	0.53	0.07	<i>discrete</i>	<b>0.04</b>	0.59	0.19
<i>circulant</i>	5.06	0.69	0.31	<i>circulant</i>	0.39	<b>0.55</b>	<b>0.38</b>	<i>circulant</i>	0.43	<b>0.59</b>	<b>0.11</b>	<i>circulant</i>	<b>0.04</b>	0.59	0.20
<i>toeplitz</i>	4.97	<b>0.71</b>	0.31	<i>toeplitz</i>	0.37	0.54	0.37	<i>toeplitz</i>	0.32	0.54	0.09	<i>toeplitz</i>	<b>0.04</b>	<b>0.60</b>	<b>0.21</b>

(i) <i>k</i> NN on MNIST				(j) <i>k</i> NN on Satellite				(k) <i>k</i> NN on Satimage-2				(l) <i>k</i> NN on Cardio			
Method	Time	ROC	P@N	Method	Time	ROC	P@N	Method	Time	ROC	P@N	Method	Time	ROC	P@N
original	7.13	<b>0.84</b>	<b>0.42</b>	original	0.71	0.67	0.49	original	0.68	0.94	<b>0.39</b>	original	0.09	0.71	0.34
PCA	3.92	<b>0.84</b>	0.40	PCA	<b>0.18</b>	0.67	0.50	PCA	<b>0.15</b>	0.94	<b>0.39</b>	PCA	<b>0.03</b>	0.73	0.34
RS	<b>3.33</b>	0.77	0.34	RS	0.31	0.68	0.49	RS	0.29	0.94	0.38	RS	<b>0.03</b>	0.69	<b>0.38</b>
<i>basic</i>	4.17	<b>0.84</b>	<b>0.42</b>	<i>basic</i>	0.24	0.68	0.49	<i>basic</i>	0.23	0.94	0.38	<i>basic</i>	<b>0.03</b>	<b>0.74</b>	0.35
<i>discrete</i>	4.11	<b>0.84</b>	0.41	<i>discrete</i>	0.25	0.69	0.50	<i>discrete</i>	0.20	0.95	0.37	<i>discrete</i>	<b>0.03</b>	<b>0.74</b>	0.37
<i>circulant</i>	4.13	<b>0.84</b>	0.41	<i>circulant</i>	0.33	<b>0.70</b>	0.50	<i>circulant</i>	0.36	<b>0.96</b>	0.37	<i>circulant</i>	<b>0.03</b>	<b>0.74</b>	0.34
<i>toeplitz</i>	4.11	<b>0.84</b>	<b>0.42</b>	<i>toeplitz</i>	0.30	<b>0.70</b>	<b>0.51</b>	<i>toeplitz</i>	0.25	<b>0.96</b>	<b>0.39</b>	<i>toeplitz</i>	<b>0.03</b>	0.73	0.35

**Table 2: Comparison between Simple scheduling and BPS against various number of base models and workers. Percent of time reduction, Redu (%), is indicated in bold.**

Dataset	<i>n</i>	<i>d</i>	<i>m</i>	<i>t</i>	Simple	BPS	Redu (%)
Cardio	1831	21	500	2	240.12	221.34	<b>7.82</b>
Cardio	1831	21	500	4	185.44	154.43	<b>16.72</b>
Cardio	1831	21	500	8	140.63	120.02	<b>14.65</b>
Cardio	1831	21	1000	2	199.77	185.63	<b>7.08</b>
Cardio	1831	21	1000	4	130.82	110.60	<b>15.45</b>
Cardio	1831	21	1000	8	97.75	73.43	<b>24.88</b>
Letter	1600	32	500	2	111.95	109.52	<b>2.17</b>
Letter	1600	32	500	4	92.69	86.24	<b>6.94</b>
Letter	1600	32	500	8	57.21	48.72	<b>14.84</b>
Letter	1600	32	1000	2	224.61	222.59	<b>0.90</b>
Letter	1600	32	1000	4	228.08	172.07	<b>24.56</b>
Letter	1600	32	1000	8	109.50	89.51	<b>17.80</b>
PageBlock	5393	10	100	2	51.11	35.17	<b>31.19</b>
PageBlock	5393	10	100	4	42.49	16.23	<b>61.80</b>
PageBlock	5393	10	100	8	38.45	16.97	<b>55.86</b>
PageBlock	5393	10	500	2	197.84	137.46	<b>30.52</b>
PageBlock	5393	10	500	4	167.36	76.14	<b>54.51</b>
PageBlock	5393	10	500	8	127.08	66.29	<b>47.84</b>
Pendigits	6870	16	500	2	351.97	287.14	<b>18.42</b>
Pendigits	6870	16	500	4	288.51	146.50	<b>49.22</b>
Pendigits	6870	16	500	8	180.86	102.11	<b>43.33</b>
Pendigits	6870	16	1000	2	697.20	561.15	<b>19.51</b>
Pendigits	6870	16	1000	4	579.70	288.11	<b>50.33</b>
Pendigits	6870	16	1000	8	365.20	182.32	<b>50.08</b>

Table 3 and 4 compare prediction performance (scoring on new-coming samples) between the original unsupervised models and pseudo-supervised approximators on 10 datasets with 6 costly algorithms. These algorithms are more computationally expensive than random forest regressors for prediction. The prediction time comparison is omitted due to space limit, but the gain is clear. Therefore, the focus is whether the approximators could predict unseen samples as good as the original unsupervised models. The tables reveal that not all the algorithms can be approximated well by supervised regressors: ABOD has a performance decrease regarding ROC on multiple datasets. ABOD is a linear models that look for a low-dimensional subspace to embed the normal samples [3], so the approximation may not work if it has extremely complex decision surfaces as mentioned before. In contrast, proximity-based models benefit from the approximation. Both table show, *k*NN, LoF, and *ak*NN (average *k*NN) experience a performance gain. Specifically, all three algorithms yield around 100% ROC increase on HTTP. Other algorithms, such as Feature Bagging and CBLOF, the ROC and PRC performances stay within the acceptable range. In other words, it is useful to perform pseudo-supervised approximation for these estimators as the time efficiency is improved at little to no loss in prediction accuracy. Through both visualization and quantitative comparisons, we believe that the proposed PSA is meaningful for offline prediction (scoring) acceleration.

**Figure 3: Decision surface comparison among unsupervised models and their pseudo-supervised counterparts. The approximator’s decision boundary shows a regularization effect over the original ones, which leads to lower errors.**

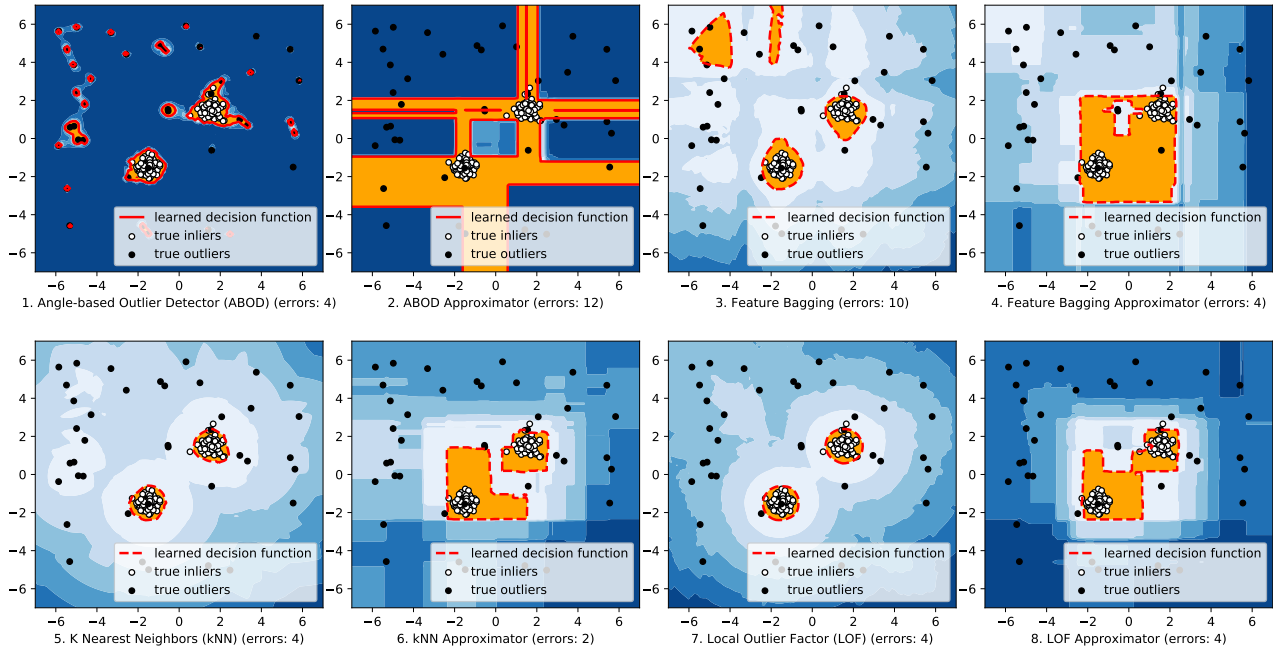


**Table 3: Test ROC scores of unsupervised models (Orig) and their pseudo-supervised approximators (Appr) by the average of 10 independent trials. The better method within each pair is indicated in bold.**

Dataset	Anthyroid		Breastw		Cardio		HTTP		MNIST		Pendigits		Pima		Satellite		Satimage-2		Thyroid	
	Orig	Appr	Orig	Appr	Orig	Appr	Orig	Appr	Orig	Appr	Orig	Appr	Orig	Appr	Orig	Appr	Orig	Appr	Orig	Appr
ABOD	<b>0.83</b>	0.71	0.92	<b>0.93</b>	<b>0.63</b>	0.53	<b>0.15</b>	0.13	<b>0.81</b>	0.79	0.67	<b>0.82</b>	0.66	<b>0.70</b>	0.59	<b>0.68</b>	0.89	<b>0.99</b>	<b>0.96</b>	0.67
CBLOF	0.67	<b>0.68</b>	0.96	<b>0.98</b>	0.73	<b>0.76</b>	<b>1.00</b>	<b>1.00</b>	0.85	<b>0.89</b>	<b>0.93</b>	<b>0.93</b>	0.63	<b>0.68</b>	0.72	<b>0.77</b>	<b>1.00</b>	<b>1.00</b>	0.92	<b>0.97</b>
FB	<b>0.81</b>	0.45	<b>0.34</b>	0.10	0.61	<b>0.70</b>	0.34	<b>0.97</b>	0.72	<b>0.83</b>	0.39	<b>0.51</b>	0.59	<b>0.63</b>	0.53	<b>0.64</b>	0.36	<b>0.40</b>	<b>0.83</b>	0.46
kNN	<b>0.80</b>	0.79	<b>0.97</b>	<b>0.97</b>	0.73	<b>0.75</b>	0.19	<b>0.85</b>	0.85	<b>0.86</b>	0.74	<b>0.87</b>	0.69	<b>0.71</b>	0.68	<b>0.75</b>	0.96	<b>0.99</b>	0.97	<b>0.98</b>
akNN	0.81	<b>0.82</b>	<b>0.97</b>	<b>0.97</b>	0.67	<b>0.72</b>	0.19	<b>0.88</b>	0.84	<b>0.85</b>	0.72	<b>0.87</b>	0.69	<b>0.71</b>	0.66	<b>0.74</b>	0.95	<b>0.99</b>	0.97	<b>0.98</b>
LOF	0.74	<b>0.85</b>	0.44	<b>0.45</b>	0.60	<b>0.68</b>	0.35	<b>0.75</b>	0.72	<b>0.76</b>	0.38	<b>0.47</b>	0.59	<b>0.65</b>	0.53	<b>0.66</b>	0.36	<b>0.38</b>	0.80	<b>0.95</b>

**Table 4: Test P@N scores of unsupervised models (Orig) and their pseudo-supervised approximators (Appr) by the average of 10 independent trials. The better method within each pair is indicated in bold.**

Dataset	Anthyroid		Breastw		Cardio		HTTP		MNIST		Pendigits		Pima		Satellite		Satimage-2		Thyroid	
	Orig	Appr	Orig	Appr	Orig	Appr	Orig	Appr	Orig	Appr	Orig	Appr	Orig	Appr	Orig	Appr	Orig	Appr	Orig	Appr
Model	Orig	Appr	Orig	Appr	Orig	Appr	Orig	Appr	Orig	Appr	Orig	Appr	Orig	Appr	Orig	Appr	Orig	Appr	Orig	Appr
ABOD	<b>0.31</b>	0.08	0.80	<b>0.83</b>	<b>0.27</b>	0.20	0.00	0.00	<b>0.40</b>	0.27	<b>0.05</b>	<b>0.05</b>	0.48	<b>0.52</b>	0.41	<b>0.46</b>	0.21	<b>0.64</b>	<b>0.36</b>	0.00
CBLOF	<b>0.25</b>	0.24	0.86	<b>0.90</b>	0.31	<b>0.34</b>	<b>0.02</b>	0.01	0.42	<b>0.48</b>	0.35	<b>0.36</b>	0.43	<b>0.48</b>	0.54	<b>0.57</b>	<b>0.96</b>	<b>0.96</b>	0.26	<b>0.38</b>
FB	<b>0.24</b>	0.02	0.03	<b>0.07</b>	0.23	<b>0.26</b>	0.02	<b>0.04</b>	0.34	<b>0.36</b>	0.03	<b>0.07</b>	0.37	<b>0.44</b>	0.37	<b>0.42</b>	0.03	<b>0.04</b>	<b>0.05</b>	0.02
kNN	0.30	<b>0.32</b>	<b>0.89</b>	<b>0.89</b>	0.37	<b>0.46</b>	<b>0.03</b>	<b>0.03</b>	0.42	<b>0.45</b>	<b>0.08</b>	0.06	<b>0.47</b>	<b>0.47</b>	0.49	<b>0.53</b>	0.32	<b>0.43</b>	0.33	<b>0.42</b>
akNN	0.30	<b>0.33</b>	0.88	<b>0.89</b>	0.34	<b>0.40</b>	<b>0.03</b>	<b>0.03</b>	0.41	<b>0.45</b>	0.05	<b>0.13</b>	0.48	<b>0.49</b>	0.47	<b>0.52</b>	0.25	<b>0.43</b>	0.31	<b>0.44</b>
LOF	0.27	<b>0.36</b>	0.19	<b>0.35</b>	<b>0.23</b>	<b>0.23</b>	0.01	<b>0.03</b>	<b>0.33</b>	0.32	0.03	<b>0.08</b>	0.40	<b>0.44</b>	0.37	<b>0.42</b>	0.04	<b>0.07</b>	0.19	<b>0.25</b>

### 4.4 Full Framework Evaluation

Table 5 shows the performance of SUOD with all three modules enabled, even not all of them are always needed in practice. In total, 600 hundred random base outlier detectors from PyOD are

trained and tested on 10 datasets. To simulate the “worst-case scenario” performance of the framework, the base detector order is randomized to minimize the intrinsic task load imbalance. In real-world applications, this order randomization may not be possible as discussed in §3.3. **Although this setting reduces the degree of**

**Table 5: Comparison between the baseline (denoted as **\_B**) and the SUOD framework (denoted as **\_S**) regarding time cost, ROC, and P@N. The better method within each pair is indicated in bold. Opendigits fail to yield meaningful P@N.**

Data Information				Time Cost (in seconds)				Ensemble Model Performance (ROC)				Ensemble Model Performance (P@N)			
Dataset	$n$	$d$	$t$	Fit_B	Fit_S	Pred_B	Pred_S	Avg_B	Avg_S	MOA_B	MOA_S	Avg_B	Avg_S	MOA_B	MOA_S
Anthyroid	7200	6	5	73.91	<b>65.23</b>	47.48	<b>44.26</b>	0.91	<b>0.93</b>	0.91	<b>0.93</b>	0.46	<b>0.54</b>	0.46	<b>0.55</b>
Anthyroid	7200	6	10	71.00	<b>42.94</b>	44.68	<b>38.66</b>	0.91	<b>0.93</b>	0.92	<b>0.93</b>	0.46	<b>0.54</b>	0.46	<b>0.54</b>
Anthyroid	7200	6	30	42.80	<b>33.98</b>	30.92	<b>25.67</b>	0.91	<b>0.93</b>	0.92	<b>0.93</b>	0.46	<b>0.54</b>	0.46	<b>0.54</b>
Cardio	1831	21	5	<b>78.84</b>	79.70	<b>46.09</b>	46.68	0.91	<b>0.93</b>	0.91	<b>0.93</b>	0.46	<b>0.54</b>	0.45	<b>0.55</b>
Cardio	1831	21	10	72.04	<b>53.43</b>	44.57	<b>38.31</b>	0.91	<b>0.93</b>	0.91	<b>0.93</b>	0.46	<b>0.54</b>	0.46	<b>0.54</b>
Cardio	1831	21	30	47.53	<b>44.57</b>	<b>31.31</b>	31.43	0.91	<b>0.93</b>	0.92	<b>0.93</b>	0.46	<b>0.54</b>	0.46	<b>0.55</b>
MNIST	7603	100	5	856.53	<b>748.40</b>	453.39	<b>324.76</b>	0.77	<b>0.81</b>	0.77	<b>0.81</b>	0.29	<b>0.35</b>	0.28	<b>0.34</b>
MNIST	7603	100	10	726.76	<b>573.66</b>	367.85	<b>328.95</b>	0.78	<b>0.81</b>	0.78	<b>0.81</b>	0.29	<b>0.35</b>	0.30	<b>0.34</b>
MNIST	7603	100	30	357.40	<b>329.71</b>	260.80	<b>134.08</b>	0.78	<b>0.81</b>	0.78	<b>0.81</b>	0.29	<b>0.35</b>	0.29	<b>0.34</b>
Optdigits	5216	64	5	295.38	<b>267.71</b>	162.28	<b>149.19</b>	0.73	<b>0.75</b>	0.75	<b>0.77</b>	0.00	0.00	0.00	0.00
Optdigits	5216	64	10	247.24	<b>224.82</b>	136.12	<b>125.54</b>	0.73	<b>0.75</b>	0.74	<b>0.75</b>	0.00	0.00	0.00	0.00
Optdigits	5216	64	30	825.23	<b>791.95</b>	110.06	<b>62.63</b>	0.73	<b>0.75</b>	0.73	<b>0.76</b>	0.00	0.00	0.00	0.00
Pendigits	6870	16	5	287.75	<b>282.25</b>	184.20	<b>158.26</b>	0.92	<b>0.95</b>	0.92	<b>0.94</b>	0.19	<b>0.23</b>	0.19	<b>0.20</b>
Pendigits	6870	16	10	281.49	<b>155.06</b>	179.83	<b>160.94</b>	0.92	<b>0.95</b>	0.92	<b>0.94</b>	0.19	<b>0.25</b>	0.19	<b>0.23</b>
Pendigits	6870	16	30	149.93	<b>145.59</b>	104.25	<b>89.85</b>	0.92	<b>0.94</b>	0.93	<b>0.94</b>	0.19	<b>0.25</b>	0.19	<b>0.22</b>
Pima	768	8	5	<b>28.72</b>	31.94	<b>21.16</b>	23.79	<b>0.71</b>	<b>0.71</b>	<b>0.71</b>	0.70	<b>0.51</b>	<b>0.51</b>	<b>0.53</b>	0.51
Pima	768	8	10	27.38	<b>20.15</b>	<b>20.81</b>	25.03	<b>0.71</b>	0.70	<b>0.71</b>	0.70	<b>0.51</b>	<b>0.51</b>	<b>0.51</b>	<b>0.51</b>
Pima	768	8	30	19.36	<b>17.89</b>	<b>13.83</b>	17.43	<b>0.71</b>	0.70	<b>0.71</b>	0.70	<b>0.51</b>	0.50	<b>0.52</b>	0.50
Shuttle	49097	9	5	3326.54	<b>1453.93</b>	2257.50	<b>1956.12</b>	<b>0.99</b>	<b>0.99</b>	<b>0.99</b>	<b>0.99</b>	<b>0.95</b>	<b>0.95</b>	<b>0.95</b>	<b>0.95</b>
Shuttle	49097	9	10	2437.10	<b>1396.21</b>	1549.97	<b>1321.16</b>	<b>0.99</b>	<b>0.99</b>	<b>0.99</b>	<b>0.99</b>	<b>0.95</b>	<b>0.95</b>	<b>0.95</b>	<b>0.95</b>
Shuttle	49097	9	30	1378.29	<b>1258.69</b>	837.41	<b>651.00</b>	<b>0.99</b>	<b>0.99</b>	<b>0.99</b>	<b>0.99</b>	<b>0.95</b>	<b>0.95</b>	<b>0.95</b>	<b>0.95</b>
SpamSpace	4207	57	5	247.98	<b>244.39</b>	130.95	<b>110.08</b>	<b>0.57</b>	0.56	<b>0.56</b>	<b>0.56</b>	<b>0.45</b>	<b>0.45</b>	<b>0.46</b>	0.45
SpamSpace	4207	57	10	233.39	<b>186.91</b>	128.24	<b>115.83</b>	<b>0.57</b>	0.56	<b>0.56</b>	<b>0.56</b>	<b>0.46</b>	0.45	<b>0.46</b>	<b>0.46</b>
SpamSpace	4207	57	30	604.00	<b>538.91</b>	70.19	<b>61.38</b>	<b>0.57</b>	0.56	<b>0.57</b>	0.56	<b>0.46</b>	<b>0.46</b>	<b>0.46</b>	0.45
Thyroid	3772	6	5	87.90	<b>71.34</b>	49.51	<b>48.20</b>	0.91	<b>0.93</b>	0.91	<b>0.93</b>	0.46	<b>0.54</b>	0.46	<b>0.55</b>
Thyroid	3772	6	10	74.76	<b>46.91</b>	44.81	<b>38.60</b>	0.91	<b>0.93</b>	0.91	<b>0.93</b>	0.46	<b>0.54</b>	0.46	<b>0.54</b>
Thyroid	3772	6	30	45.84	<b>43.86</b>	28.90	<b>26.75</b>	0.91	<b>0.93</b>	0.92	<b>0.93</b>	0.46	<b>0.54</b>	0.46	<b>0.54</b>
Waveform	3443	21	5	167.98	<b>147.00</b>	109.94	<b>94.46</b>	<b>0.78</b>	0.76	<b>0.78</b>	0.76	0.11	<b>0.13</b>	0.11	<b>0.13</b>
Waveform	3443	21	10	154.72	<b>94.36</b>	91.69	<b>55.17</b>	<b>0.78</b>	0.76	<b>0.78</b>	0.77	<b>0.11</b>	<b>0.11</b>	<b>0.11</b>	<b>0.11</b>
Waveform	3443	21	30	97.11	<b>95.77</b>	53.47	<b>48.04</b>	<b>0.78</b>	0.76	<b>0.78</b>	0.76	0.11	<b>0.13</b>	0.11	<b>0.13</b>

**time reduction of the BPS module, we choose it to provide an empirical worst-case performance guarantee—the framework should surely perform better in practice.**

SUOD consistently yields promising results even we deliberately choose the unfavour setting. **Fit\_B** and **Pred\_B** denote the fit and prediction time of the baseline setting (no projection, no approximation, simple parallel task scheduling; see §2.2). In comparison, SUOD (denoted as **Fit\_S** and **Pred\_S**) brings time reduction on majority of the datasets with minor to no performance degradation. To measure the prediction performance, we measure the ROC and P@N by averaging the base model results (denoted as **Avg\_**) and the maximum of average of the base models (denoted as **MOA\_**), a widely used two-phase outlier score combination framework [4]. Surprisingly, SUOD leads to small performance boost in scoring new samples on most of the datasets (**Anthyroid**, **Cardio**, **MNIST**, **Optdigits**, **Pendigits**, and **Thyroid**). This performance gain may be jointly credited to the regularization effect by the randomness injected in JL projection (§3.1) and the pseudo-approximation (§3.2)—the baseline setting may be overfitted on certain datasets. It is noted that SUOD leads to more improvement on high-dimensional, large datasets. For instance, the fit time is significantly reduced on **Shuttle**. On the contrary, SUOD is less useful for small datasets like **Pima** and **Cardio**, although they may also yield performance improvement. It is also interesting to notice for majority of the datasets,

the most significant time reduction happens with the number of cores  $t = 10$ . Indeed, the absolute value of  $t$  is less meaningful, as the effect also depends on the number of base detectors. In our experiment setting,  $t = 5$  discounts the effect of BPS because the detector order is already randomized, while  $t = 30$  will not benefit too much from BPS as each worker only needs to handle 20 detectors. This suggests larger performance gain may be achieved by selecting an appropriate number of workers for the base detectors.

#### 4.5 Real-World Deployment Case: Fraudulent Medical Claim Analysis at IQVIA

Estimated by the United States Government Accountability Office and Federal Bureau of Investigation, healthcare frauds cost American taxpayers tens of billions dollars a year [6, 7]. Detecting fraudulent medical claims is crucial for taxpayers, pharmaceutical companies and insurance companies. To further demonstrate SUOD’s performance on industry data, we deploy it on a proprietary pharmacy claim dataset owned by IQVIA consisting of 123,720 medical claims among which 19,033 (15.38%) are labeled as fraudulent. In each of the claim, there are 35 features including information such as drug brand, copay amount, insurance details, location and pharmacy/patient demographics. The current system in use is based on a group of selected detection models in PyOD, and an averaging



method is applied on top of the base model results as the initial result. The cases marked as high risk are then transferred to human investigators in special investigation unit (SIU) for verification. It is important to provide prompt and accurate first-round screening for SIU, which leads to huge expense save.

SUOD is applied on top of the aforementioned dataset (74,220 records are used for training and 49,500 records are set aside for validation). Similarly to the full framework evaluation in §4.4, the new system with SUOD (all three modules enabled) is compared with the current distributed system on 10 cores. The fit time is reduced from 6232.54 seconds to 4202.30 seconds (32.57% reduction), and the prediction time is reduced from 3723.45 seconds reduced to 2814.92 seconds (24.40%). In addition to the time reduction, ROC and P@N also shows an improvement at 3.59% and 7.46%, respectively. Through this case, we are confident the proposed framework can be useful for many real-world applications for scalable learning.

## 5 CONCLUSION & FUTURE DIRECTIONS

In this work, a three-module framework called SUOD is proposed to accelerate the training and prediction with a large number of unsupervised outlier detectors. The three modules in SUOD focus on different levels (data, model, system): (i) Random Projection module generates low-dimensional subspaces to alleviate the curse of dimensionality using toeplitz Johnson-Lindenstrauss projection; (ii) Pseudo-supervised Approximation module could accelerate costly unsupervised models' prediction speed by replacing them by scalable supervised regressors, which also brings the extra benefit regarding interpretability and storage cost and (iii) Balanced Parallel Scheduling module ensures that nearly equal amount of workload is assigned to multiple workers in parallel training and prediction. The extensive experiments on more than 20 benchmark datasets and a real-world claim fraud analysis case show the great potential of SUOD, and many intriguing results are observed. For model reproducibility and accessibility, the framework, all code, figures, and datasets are openly shared<sup>1</sup>.

Many investigations are underway. First, we would like to demonstrate SUOD's effectiveness as an end-to-end framework on more complex combination models like unsupervised LSCP [35] and XG-BOD [34]. Second, we would further emphasize the interpretability provided by the pseudo-supervised approximation, which can be beyond simple feature importance provided in tree regressors. Third, we see there is room to investigate why and how the pseudo-supervised approximation could work in a more strict and theoretical way. Specifically, we want to know how to choose supervised regressors and under what conditions the approximation could work. This study, as the first step, empirically shows that proximity-based models benefit from the approximation, whereas linear models may not. Fourth, other classical acceleration methods may be explored as well, e.g., using low numeric precision. Lastly, it is interesting to extend and generalize SUOD to other unsupervised tasks, such as streaming-based outlier detection and clustering ensemble.

## REFERENCES

- [1] Dimitris Achlioptas. 2001. Database-friendly random projections. In *PODS*. ACM.
- [2] Charu C Aggarwal. 2013. Outlier ensembles: position paper. *ACM SIGKDD Explorations Newsletter* 14, 2 (2013), 49–58.
- [3] Charu C Aggarwal. 2016. *Outlier Analysis*. Springer.
- [4] Charu C. Aggarwal and Saket Sathé. 2017. *Outlier ensembles: An introduction* (1st ed.). Springer. 1–276 pages.
- [5] Leman Akoglu, Rishi Chandy, and Christos Faloutsos. 2013. Opinion fraud detection in online reviews by network effects. In *ICWSM*.
- [6] N Aldrich, J Crowder, and B Benson. 2014. How much does medicare lose due to fraud and improper payments each year. *The Sentinel* (2014).
- [7] S. J. Bagdoyan. 2018. MEDICARE: Actions Needed to Better Manage Fraud Risks. <https://www.gao.gov/assets/700/693156.pdf> (2018).
- [8] Leo Breiman. 2001. Random forests. *Machine learning* 45, 1 (2001), 5–32.
- [9] Markus M. Breunig, Hans-Peter Kriegel, Raymond T. Ng, and Jörg Sander. 2000. LOF: Identifying Density-Based Local Outliers. *SIGMOD* (2000), 1–12.
- [10] Varun Chandola, Arindam Banerjee, and Vipin Kumar. 2009. Anomaly detection: A survey. *CSUR* 41, 3 (2009), 15.
- [11] Geoffrey Hinton, Oriol Vinyals, and Jeff Dean. 2015. Distilling the knowledge in a neural network. *arXiv preprint arXiv:1503.02531* (2015).
- [12] Jianying Hu, Fei Wang, Jimeng Sun, Robert Sorrentino, and Shahram Ebadollahi. 2012. A healthcare utilization analysis framework for hot spotting and contextual anomaly detection. In *AMIA annual symposium proceedings*.
- [13] Xiyang Hu, Cynthia Rudin, and Margo Seltzer. 2019. Optimal Sparse Decision Trees. *NeurIPS* (2019), 7265–7273.
- [14] William B Johnson and Joram Lindenstrauss. 1984. Extensions of Lipschitz mappings into a Hilbert space. *Contemporary mathematics* 26, 189–206 (1984), 1.
- [15] Fabian Keller, Emmanuel Muller, and Klemens Böhm. 2012. HiCS: High contrast subspaces for density-based outlier ranking. In *ICDE*.
- [16] Hans-Peter Kriegel, Peer Kröger, Erich Schubert, and Arthur Zimek. 2009. LoOP: local outlier probabilities. *CIKM* (2009), 1649–1652.
- [17] Aleksandar Lazarevic, Levent Ertoz, Vipin Kumar, Aysel Ozgur, and Jaideep Srivastava. 2003. A comparative study of anomaly detection schemes in network intrusion detection. In *SDM*. 25–36.
- [18] Aleksandar Lazarevic and Vipin Kumar. 2005. Feature bagging for outlier detection. In *KDD*. ACM, 157–166.
- [19] Wenyuan Li, Yunlong Wang, Yong Cai, Corey Arnold, Emily Zhao, and Yilian Yuan. 2018. Semi-supervised Rare Disease Detection Using Generative Adversarial Network. In *NeurIPS Workshop*.
- [20] Fei Tony Liu, Kai Ming Ting, and Zhi-Hua Zhou. 2008. Isolation forest. In *ICDM*.
- [21] Yezheng Liu, Zhe Li, Chong Zhou, Yuanchun Jiang, Jianshan Sun, Meng Wang, and Xiangnan He. 2019. Generative adversarial active learning for unsupervised outlier detection. *TKDE* (2019).
- [22] Elio Lozano and E Acufia. 2005. Parallel algorithms for distance-based and density-based outliers. In *ICDM*.
- [23] Weining Lu, Yu Cheng, Cao Xiao, Shiyu Chang, Shuai Huang, Bin Liang, and Thomas Huang. 2017. Unsupervised sequential outlier detection with deep architectures. *IEEE Transactions on Image Processing* 26, 9 (2017), 4321–4330.
- [24] Barbora Mícenková, Brian McWilliams, and Ira Assent. 2014. Learning outlier ensembles: The best of both worlds—supervised and unsupervised. In *SIGKDD Workshop*. 51–54.
- [25] Junki Oku, Keichi Tamura, and Hajime Kitakami. 2014. Parallel processing for distance-based outlier detection on a multi-core CPU. In *IEEE International Workshop on Computational Intelligence and Applications (IWCI/A)*. IEEE, 65–70.
- [26] Fabian Pedregosa, Gaël Varoquaux, Alexandre Gramfort, Vincent Michel, Bertrand Thirion, Olivier Grisel, Mathieu Blondel, Peter Prettenhofer, Ron Weiss, et al. 2011. Scikit-learn: Machine learning in Python. *JMLR* (2011).
- [27] Sridhar Ramaswamy, Rajeev Rastogi, K. Shim, Murray Hill, Kyuseok Shim, and Kyuseok Sim Ramaswamy, Sridhar, Rajeev rastogi. 2000. Efficient algorithms for mining outliers from large data sets. *ACM SIGMOD Record* 29, 2 (2000), 427–438.
- [28] Shebuti Rayana and Leman Akoglu. 2016. Less is more: Building selective anomaly ensembles. *TKDD* 10, 4 (2016), 42.
- [29] Erich Schubert, Arthur Zimek, and Hans-Peter Kriegel. 2015. Fast and scalable outlier detection with approximate nearest neighbor ensembles. In *DASFAA*.
- [30] Mei-Ling Shyu, Shu-Ching Chen, Kanoksri Sarinnapakorn, and LiWu Chang. 2003. *A novel anomaly detection scheme based on principal component classifier*. Technical Report.
- [31] C Spearman. 1904. The proof and measurement of association between two things. *AJP* (1904).
- [32] Suresh Venkatasubramanian and Qiushi Wang. 2011. The Johnson-Lindenstrauss transform: an empirical study. In *ALLENEX Workshop*. SIAM, 164–173.
- [33] Yue Zhao, Xueying Ding, Jianing Yang, and Haoping Bai. 2020. SUOD: Toward Scalable Unsupervised Outlier Detection. In *AAAI Workshops*.
- [34] Yue Zhao and Maciej K Hryniewicki. 2018. XGBOD: Improving Supervised Outlier Detection with Unsupervised Representation Learning. In *IJCNN*. IEEE.
- [35] Yue Zhao, Zain Nasrullah, Maciej K Hryniewicki, and Zheng Li. 2019. LSCP: Locally Selective Combination in Parallel Outlier Ensembles. In *SDM*. 585–593.
- [36] Yue Zhao, Zain Nasrullah, and Zheng Li. 2019. PyOD: A Python Toolbox for Scalable Outlier Detection. *JMLR* 20, 96 (2019), 1–7.
- [37] Arthur Zimek, Ricardo JGB Campello, and Jörg Sander. 2014. Ensembles for unsupervised outlier detection: challenges and research questions a position paper. *ACM SIGKDD Explorations Newsletter* 15, 1 (2014), 11–22.

<sup>1</sup><https://github.com/yzhao062/SUOD>

## APPENDIX: REPRODUCIBILITY

### A DATASETS, EVALUATION METRICS & IMPLEMENTATION

Table 1 describes the selected outlier detection benchmark datasets, and more than 20 outlier detection benchmark datasets are used in this study<sup>1,2</sup>. The data size  $n$  varies from 452 (**Arrhythmia**) to 567,479 (**HTTP**) samples and the dimension  $d$  ranges from 3 to 274. For both random projection and parallel scheduling experiments, the full datasets are used for model building (training). For the pseudo-supervised approximation experiments and the full framework assessment, 60% of the data is used for training and the remaining 40% is set aside for validation. For all experiments, performance is evaluated by taking the average of 10 independent trials using area under the receiver operating characteristic (ROC) curve and precision at rank  $n$  (P@N)—here  $n$  denotes the actual number of outliers. Both metrics are widely used in outlier research [21, 37].

In this study, unsupervised models are taken from the major outlier mining library—Python Outlier Detection Toolbox (PyOD) [36]. Supervised regressors and utility functions are based on standard libraries (scikit-learn and numpy). For a fair comparison, none of the models involve parameter tuning process. Two machines (#1: Intel i7-9700 @ 3.00 GHZ, 32 GB RAM, 8 cores; #2 (Intel Xeon E7-4830 @ 2.10 GHZ, 1 TB RAM, 96 cores) are used for consistency.

**Table 1: Selected real-world benchmark datasets**

Dataset	Pts ( $n$ )	Dim ( $d$ )	Outliers	% Outlier
Annthyroid	7200	6	534	7.41
Arrhythmia	452	274	66	14.60
Breastw	683	9	239	34.99
Cardio	1831	21	176	9.61
HTTP	567479	3	2211	0.40
Letter	1600	32	100	6.25
MNIST	7603	100	700	9.21
Musk	3062	166	97	3.17
PageBlock	5393	10	510	9.46
Pendigits	6870	16	156	2.27
Pima	768	8	268	34.90
Satellite	6435	36	2036	31.64
Satimage-2	5803	36	71	1.22
seismic	2584	10	170	6.59
Shuttle	49097	9	3511	7.15
SpameSpace	4207	57	1679	39.91
speech	3686	400	61	1.65
Thyroid	3772	6	93	2.47
Vertebral	240	6	30	12.50
Vowels	1456	12	50	3.43
Waveform	3443	21	100	2.90
Wilt	4819	5	257	5.33

<sup>1</sup>ODDS Library: <http://odds.cs.stonybrook.edu>

<sup>2</sup>DAMI Datasets: <http://www.dbs.ifi.lmu.de/research/outlier-evaluation/DAMI>